Journal of Molecular Graphics and Modelling 44 (2013) 188–196

Contents lists available at ScienceDirect

Journal of Molecular Graphics and Modelling

journal homepage: www.elsevier.com/locate/JMGM

Similarity-based virtual screening for microtubule stabilizers reveals novel antimitotic scaffold

Ahmed T. Ayoub[a], Mariusz Klobukowski[a], Jack Tuszynski[b,*]

[a] Department of Chemistry, University of Alberta, Edmonton, AB, Canada
[b] Department of Physics, University of Alberta, Edmonton, AB, Canada

ARTICLE INFO

Article history:
Received 13 February 2013
Received in revised form 25 May 2013
Accepted 27 May 2013
Available online 25 June 2013

Keywords:
Tubulin
Virtual screening
MM/PBSA
Microtubule stabilizing agents

ABSTRACT

Microtubules are among the most studied and best characterized cancer targets identified to date. Many microtubule stabilizers have been introduced so far that work by disrupting the dynamic instability of microtubules causing mitotic block and apoptosis. However, most of these molecules, especially taxol and epothilone, suffer absorption, toxicity and/or resistance problems. Here we employ a novel similarity-based virtual screening approach in the hope of finding other microtubule stabilizers that perform better and have lower toxicity and resistance. Epothilones, discodermolide, eleutherobin and sarcodictyin A have been found to compete with taxanes for the β-tubulin binding site, which suggests common chemical features qualifying for that. Our approach was based on similarity screening against all these compounds and other microtubule stabilizers, followed by virtual screening against the taxol binding site. Some novel hits were found, together with a novel highly rigid molecular scaffold. After visual manipulations, redocking and rescoring of this novel scaffold, its affinity dramatically increased in a promising trend, which qualifies for biological testing.

1. Introduction

Cancer, a major cause of death in the world [1], is characterized by uncontrolled growth of cells within certain tissues that could spread to other tissues through metastasis. The apparent immortality and uncontrolled division of cells is one of the hallmarks of cancer and it can be overcome by chemotherapy which targets these rapidly dividing cells with cytotoxic chemical agents [2]. One of the most important drug targets in this context is the structural protein tubulin, the building block of microtubules. Microtubules are long filamentous tube-shaped protein polymers required in cells, among numerous other roles, for transport of vesicles and structural support [3]. During the anaphase of the mitotic division, microtubules play the role of separating chromosomes to the poles of cell preceding telophase. Proper dynamics of microtubules, in terms of the delicate balance between catastrophe and rescue phases, are crucial for these mitotic phases to complete [3]. Taxol and other anticancer microtubule stabilizing agents (MSAs) work by stabilizing the microtubules and thus disrupting their required dynamic instability, which leads to mitotic arrest followed by apoptosis [4,5]. The binding site of taxol was correctly identified to be in the β-tubulin of the $\alpha\beta$-tubulin heterodimer and was elucidated via electron crystallography and photoaffinity labeling [6–8]. Among the recognized MSAs are also epothilone, discodermolide, sarcodictyin and eleutherobin, all of which have been shown to compete with taxol for the β-tubulin binding site [9–12]. Also, laulimalide, which is an MSA, was shown to have affinity toward the taxol binding site [13,14] but its primary binding location has been shown to differ from that for taxol [15]. Fig. 1 shows the two-dimensional structures of these molecules. Most of these MSAs, however, suffer from some solubility, toxicity and/or drug resistance problems [16–19] revealed in pre-clinical and clinical trials. This strongly motivates the search for novel tubulin-binding agents that may be able to provide a better pharmacokinetic profile and evade the resistance caused by mutations or cellular efflux pumps. Several studies have been conducted to find out a common pharmacophore for the MSAs that compete with taxol for the binding site and some models have been presented [20–22]. However, the lack of definitive data regarding the bioactive conformation of some of these ligands, besides the high structural complexity of most of them poses some questions regarding the reliability of these pharmacophore models in virtual screening. Therefore, we employed another approach in this study, which is the similarity-based approach, for filtering large sets of molecules, instead of the pharmacophore approach. We also employed docking and virtual screening techniques supported by Tanimoto similarity [23] in the hope of finding new scaffolds for tubulin-binding agents that can strongly bind to the taxol binding site whilst having better molecular properties.

* Corresponding author. Tel.: +1 780 432 8906.
E-mail addresses: jackt@ualberta.ca, jack.tuszynski@gmail.com (J. Tuszynski).

1093-3263/$ – see front matter © 2013 Elsevier Inc. All rights reserved.
http://dx.doi.org/10.1016/j.jmgm.2013.05.008

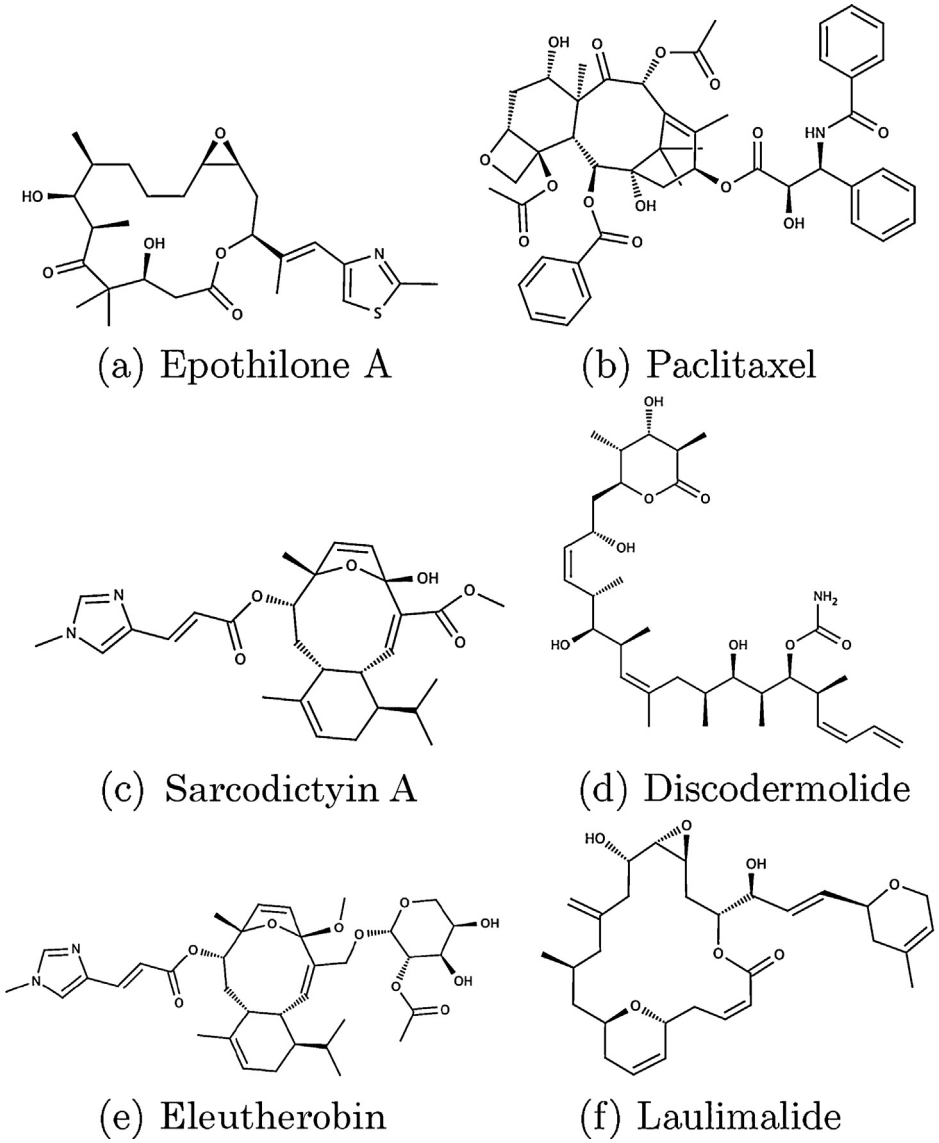

Fig. 1. Different MSAs that have affinity toward the the taxol binding site on β-tubulin.

2. Materials and methods

2.1. Filtering PubChem Compound Library

As explained earlier, paclitaxel, epothilone A, discodermolide, sarcodictyin A, eleutherobin and laulimalide all have affinities toward the taxol binding site [9–14]. Based on that, we considered the ensemble of chemical features represented in these molecules as being representative of most of the chemical features required for binding to the taxol binding site. Hence, similarity with any of these six compounds was used as a criterion for filtering the compound database. The PubChem compound library, which is composed of nearly 33 million chemical entities, was screened against each of these six compounds separately to filter all the molecules that are at least 80% similar to the query molecules based on the Tanimoto coefficient similarity metric [23]. The filtered molecules were then subjected to another filtering step based on Lipinski's rule of five that is widely accepted as a criterion from a pharmacological usefulness viewpoint [24]. The filtered molecules based on the six query structures were then combined together to give a library of 1591 molecules. Duplicates were deleted, the library was clustered and a diversity subset was selected based on 90% Tanimoto similarity to avoid having to evaluate molecules that are almost identical in structure. We ended up creating a library of 645 molecules that satisfy all of the above criteria and are ready for docking. We have added epothilone A as positive control. The 646 molecules were then docked into the taxol binding site using AutoDock 4.2 [25]. Details of the filtration process are depicted in Fig. 2. The Lamarckian genetic algorithm, which is a hybrid genetic algorithm with local search, was used for docking, with a maximum of 3 million runs of energy evaluations in a population size of 500 and a maximum of 50,000 generations. Docking poses were clustered based on a root-mean-square tolerance of 2.0 Å and the results were ranked based on the lowest energy in the largest cluster.

The 25 top hits were assessed for novelty of the scaffold and the best candidate was modified visually. MarvinSketch 5.10.3, 2012 (ChemAxon) was used for drawing, displaying and characterizing chemical structures. Avogadro 1.0.3 was also used to assist in visualization and for energy minimization of the structures prior to docking [26]. The best candidate from the virtual screening run was modified and several functional groups were added to different sites in the molecule to optimize the ligand–receptor complex based on visual inspection of the complex structure. The modified

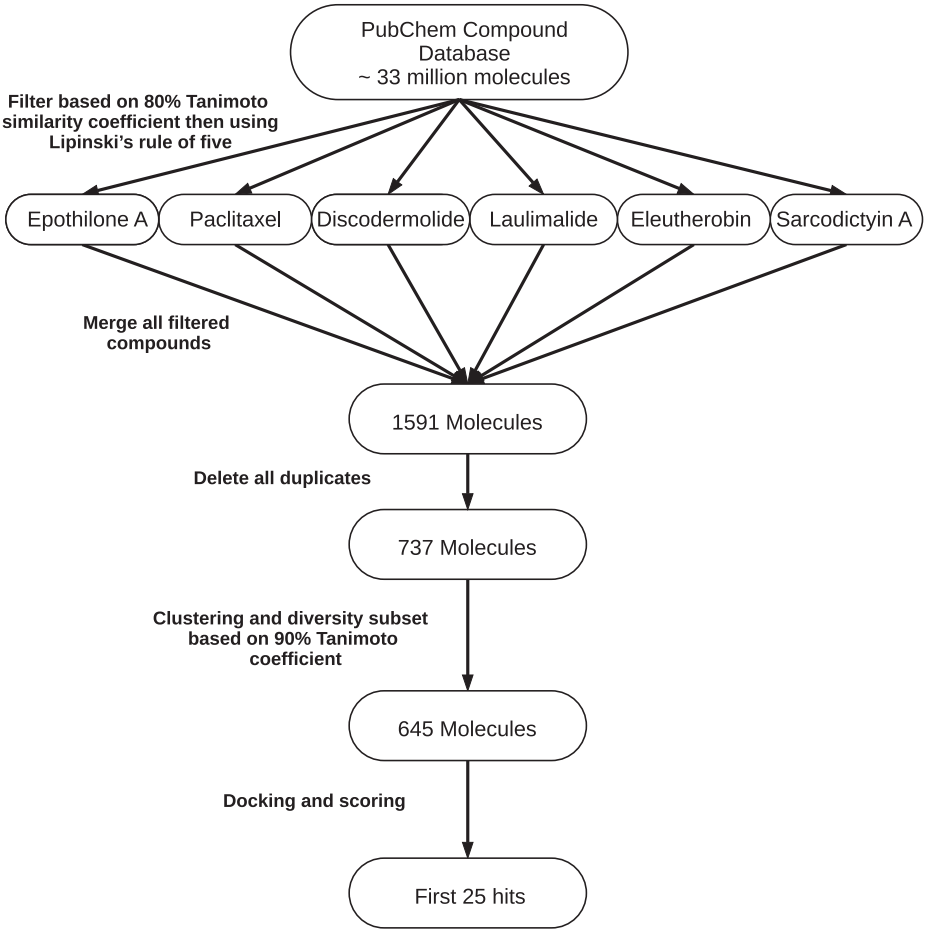

Fig. 2. Filtration scheme of the PubChem Compound Library of ~33 million molecules preceding docking.

molecules were then redocked into the taxol binding site. The visual modification and redocking steps were repeated five times until the derivatives showed highest affinity and no further improvements were being generated. Hybridization between the best scoring hits in each run was utilized to optimize the results in the subsequent run.

2.2. Preparing receptor for docking

The receptor, tubulin, was obtained from the crystal structure 1TVK from the Protein Data Bank. 1TVK was preferred over 1JFF and 1TUB because of its high resolution (2.89 Å as compared to 3.50 Å and 3.70 Å, respectively). The molecule was minimized using AMBER 12 [27] to relieve any unfavorable interactions that may result from crystal packing. The receptor was parameterized according to the AMBERff99SB force field [28]. Hydrogen atoms were added to the protein based on the built-in AMBER residue templates, missing fragments were capped and residue HIS^{227} was kept in the deprotonated state [29]. The Antechamber module of AMBER 12 package was used for parameterizing the ligands (epothilone, GDP and GTP) via the general AMBER force field [30] and atomic partial charges were assigned using the AM1-BCC method [31]. The complex was built using the *tleap* module of AMBER which was also used to neutralize the complex by addition of counterions and to solvate the system using a truncated octahedral box of the TIP3P water model that extended 12 Å in each direction. The model was minimized using AMBER 12 in a series of steepest descent and conjugate gradient steps. The minimized structure was then processed for docking; the α-tubulin subunit was deleted together with the solvent and all the ligands as they play no role in binding to the identified location on β-tubulin. Only the β-subunit was used for docking, at the epothilone binding site, which is the same as the taxane binding site. AutoDock Tools 4.2 was used to process the receptor [25]. The grid box for docking was centered around the crystallized epothilone structure in the binding site of 1TVK and was given the dimensions of $58 \times 58 \times 58$ grid points and was ready for docking. The software VMD was used for the visualization of molecular dynamics trajectories in all of our work in this paper [32].

2.3. Rescoring the best hits using MM/PBSA

Five of the six query molecules that were used for the similarity-based filtering (see Fig. 2) plus three of the highest-scoring hits that were obtained from the consecutive modification/redocking runs had their binding energies rescored using molecular mechanics Poisson–Boltzmann surface area (MM/PBSA) approach that was introduced by Kollman et al. [33]. This approach has been applied successfully in predicting the binding energies of many protein–ligand complexes [34–38]. Building on the success of these previous trials, we first rescored the five test molecules that interact with the taxol binding site with available experimental binding energies, namely discodermolide, eleutherobin, epothilone A, paclitaxel and sarcodictyin A, to verify the predictive power of the method through a linear fit. We neglected laulimalide because there was no available experimental data regarding its binding to the taxol binding site. Then we ran the same protocol with the highest-scoring hits to confirm the ranking as well as the binding energies

predicted by the docking algorithm. To summarize the MM/PBSA approach, a molecular dynamics simulation is usually run in solvent and in the presence of counterions to obtain an equilibrated system of the ligand–receptor complex. A set of uncorrelated snapshots of the trajectories are post-processed by removal of the solvent and counterions. The average free energy of each species, ligand, receptor or complex, is calculated according to the following equation:

$$\overline{G} = \overline{E}_{MM} + \overline{G}_{PBSA} - TS_{MM} \quad (1)$$

where $\overline{E}_{MM}$ is the average molecular mechanical energy calculated according to this equation:

$$\overline{E}_{MM} = \overline{E}_{bond} + \overline{E}_{angle} + \overline{E}_{tors} + \overline{E}_{vdw} + \overline{E}_{elec} \quad (2)$$

where all these contributions correspond to the calculated force field values of bond, angle, torsional, van der Waals and electrostatic terms. The term $\overline{G}_{PBSA}$ in Eq. (1) refers to the solvation free energy obtained from the Poisson–Boltzmann equation and an estimate for the non-polar free energy via a surface area term. The term $-TS_{MM}$ is the entropy contribution which can be calculated via either quasi harmonic approximation or normal mode analysis. After calculating the average free energies for the ligand, the receptor and the complex, the total average free energy of binding in solution equals [33]:

$$\Delta G = \overline{G}_{complex} - \overline{G}_{receptor} - \overline{G}_{ligand} \quad (3)$$

Toward this end, all the ligand–receptor complexes were subjected to molecular dynamics simulation to obtain an equilibrated system. We used only the β-tubulin subunit for the simulations because the α subunit is not involved in binding, and to save computational time. The simulations were performed using AMBER 12 package [27] following the same procedures as described in Section 2.2. The GDP molecule that is normally attached to β-tubulin in the 1TVK structure was also parameterized following the same approach as other ligands and was docked into its binding site when forming the complexes to make the model as realistic as possible. The ligand–receptor complexes were built using the *tleap* module of AMBER and were solvated with a truncated octahedral box of TIP3P water model extending 12 Å in each direction. The charge was neutralized by the addition of 18 sodium ions and then 22 sodium and chloride ions were added to adjust the ion concentration to 100 mM which mimics cellular conditions. Each complex was then minimized without SHAKE on hydrogen and with very strong restraints on the protein through 500 steepest descent runs followed by 500 conjugate gradient steps. This was to relieve any unfavorable hydrogen contacts caused the addition of hydrogen by *tleap*. Then, the complexes were minimized once more without restraints nor SHAKE through 2000 steps of steepest descent followed by 2000 steps of conjugate gradient to remove any other unfavorable contacts. The complexes were then subjected to 20 ps of heating using Langevin thermostat to 300 K at constant volume under SHAKE and restraints on the protein. This was followed by 200 ps of density equilibration at constant pressure with SHAKE on hydrogen but without restraints on the protein. Each complex was then taken through a production phase of 11 ns under constant pressure with the same settings as the previous density equilibration step. All the simulations were performed under periodic boundary conditions using Particle–Mesh–Ewald method for treating long-range electrostatics and Langevin thermostat for temperature control. Coordinates were recorded every 2 ps in the production run to ensure that the snapshots are uncorrelated. Total energy, temperature, density and RMSD of the complexes were then checked for equilibration. Complexes were then subjected to an MM/PBSA calculation in AMBER 12 to calculate the binding enthalpy under an ionic strength of 100 mM and an internal and external dielectric constants of 1.0 and 80.0, respectively. Although computationally very demanding, the entropies of the solutes were estimated using normal mode analysis in order to be able to calculate the total ΔG of the molecules and compare them to available experimental values as a check of the predictive power of the method in reproducing experimental data and hence being reliable in predicting the binding energy of the newly proposed ligands.

2.4. Prediction of physicochemical properties

The compounds that showed high affinities during the docking/rescoring runs were checked for their physicochemical parameters. ADMET Predictor software [39] was used for calculation of parameters such as partition coefficient ($\log P$), distribution coefficient ($\log D$), effective human jejunal permeability (P_{eff}) and solubility in simulated intestinal fluid in fasted state (FaSSIF). Potential toxicity was also assessed by the same software.

3. Results and discussion

3.1. Results of virtual screening

As described previously in Fig. 2, the similarity-based filtering of the ~33 million molecules yielded 645 molecules. These molecules, together with epothilone A used as a positive control, were docked in β-tubulin as described in Section 2.1. After ranking the docking results based on the lowest energy of the largest cluster, the best-scoring 25 molecules were examined. Before listing the results, it is worth mentioning that most of the highest scoring molecules are expected to be well-known and probably patented molecules. The approach that we are following, i.e. the similarity approach, retains molecules that are similar to active ones, including their patented analogs. If these analogs occur on top of the list, this is expected. Our main objective it to identify novel scaffolds, among these top hits, that can be modified to generate better ligands. The virtual screening algorithm predicted the first 25 hits to be strong tubulin-binders spanning a binding energy from −10.03 kcal/mol for the best hit (ligand PubChem CID of 10718437) to −9.02 kcal/mol for the worst one (ligand CID of 643649). To prove the efficiency of the docking algorithm in predicting active molecules, we will discuss the first five hits. From SciFinder, we found that the best hit, with CAS Registry Number of 198475-16-0, is an epothilone analog that was shown by Su et al. to have efficacy against cancer cell lines as a microtubule stabilizer [40]. The second hit, CAS 219990-00-8, also has an activity against tubulin, similar to that of epothilone, and was patented by Vite et al. (patent number WO 9902514) and Francis Lee (WO 2002066038) for treatment of hyperproliferative cellular disease and refractory tumors, respectively. The third hit, which is a laulimalide analog with CAS of 1049737-16-7, was shown by Mooberry et al. to possess potent antiproliferative activity due to microtubule stabilization [41]. The fourth hit, CAS 220889-57-6, is an epothilone analog proven active by Lam et al. [42]. Finally, the fifth hit, CAS 252917-46-7, was shown by Hardt et al. to be a potent epothilone analog [43]. In fact, all the top 25 hits, except for five novel ligands, represent compounds that have experimentally been shown to have tubulin stabilizing activities, which proves the reliability of our docking algorithm in determining active molecules. The five novel hits found in virtual screening are presented in Table 1 and compared to the positive control, epothilone A. The first of these five molecules, molecule 53 (CID 44333743), was shown by Sefkow et al. to have weak cytotoxic activity against the L 929 mouse fibroblast cell line, but was not patented [44]. Molecule 70 (CID 23242270) and 84 (CID 20822803) were not yet shown, experimentally, to have binding affinity toward tubulin. However, these three molecules have obvious similarity to the epothilone scaffold (molecule 44) and hence represent no new scaffold for us to adopt. Molecule 118

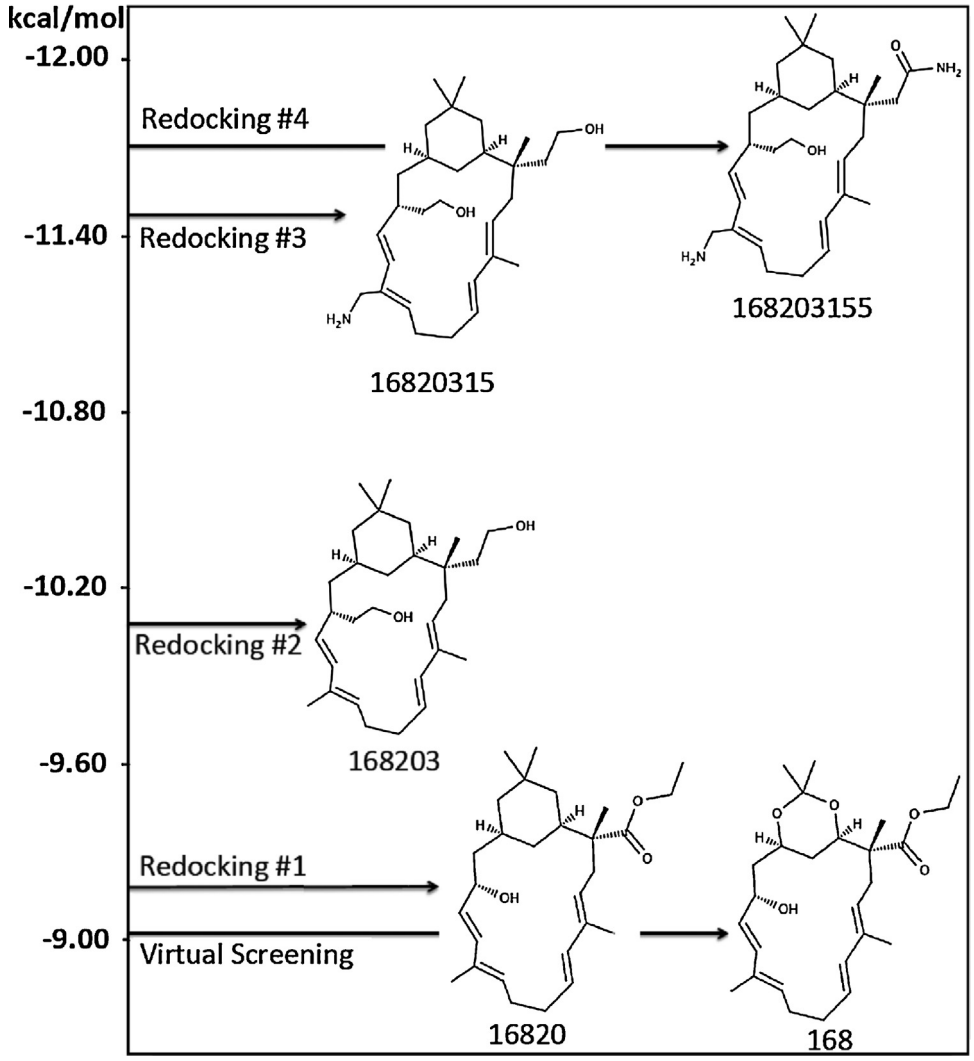

Fig. 3. The quantitative improvement of the binding energies (on the *y*-axis) of the top hits obtained in each of the consecutive modification/redocking runs on molecule 168.

(CID 10625150) is 12,13-deoxyroridin E which is produced by the marine-derived fungus *Myrothecium roridum* and was shown by Namikoshi et al. to have cytotoxicity against human (HL-60) and murine (L1210) leukemia cell lines but as of writing this paper has not yet been patented as an anticancer tubulin-binding agent [45]. This all shows that the protocol was strong enough in separating active from non-active molecules, with most of the strongly active molecules appearing on top of the list. The most attractive molecule is molecule 168 (CID 10477941) for it represents a completely new scaffold in this category of compounds. Not only is the scaffold entirely new, but its structure is much simpler than many tubulin binders and appears to be very rigid. Due to its promising characteristics, we decided to undertake further optimization runs for this molecule through modification and redocking. As described in Section 2.1, we modified molecule 168 by addition of several functional groups to different positions in the molecule. The modification was based on visual inspection of the binding mode of molecule 168 to tubulin and on trying to optimize binding and the hydrogen bond network. We ran this modification/redocking step four consecutive times till the derivatives showed best affinity and no further improvements were obtained. Fig. 3 shows the top hits from each run and shows the trend of the improvement of the binding affinity following our modification/redocking protocol. It is clear that this protocol managed to bring molecule 168 from a binding affinity of −9.03 kcal/mol to a binding affinity of −11.76 kcal/mol (molecule 168203155) which is much higher than the top hit obtained in the first virtual screening run (molecule 38 with a binding energy of −10.03 kcal/mol). However, these hits that we obtained appear to be highly lipophilic and their water solubility, and absorption could be questioned. These are serious drawbacks in the context of chemotherapy applications. Therefore, we decided to run another modification/redocking run on the best hit, molecule 168203155, with the purpose of only increasing the hydrophilicity of the derivatives, while still maintaining a good affinity.

Table 2 shows the result of this fifth run with the corresponding binding energies of each derivative. It shows that we could not get any derivative to be any better than the parent molecule, molecule 168203155, in terms of binding energy. However, their binding energies are still in the top range and we managed to increase their hydrophilicity by the inclusion of hydrophilic functional groups. It is worth mentioning that all the derivatives of molecule 168 are very rigid and there is only one mode of binding available for these molecules in the tubulin binding site. Within an RMSD of 2.00 Å, nearly all the binding poses would group in one cluster. This rigidity can be exploited in tailor designing analogs that are more selective toward certain tubulin isoforms over the others, thus increasing the specificity of the treatment. Fig. 4(a)

Table 1
The binding energies of the five novel hits obtained in the virtual screening run, plus the positive control, epothilone A.

Rank	ID[a]	Molecule	ΔE[b]
6	53	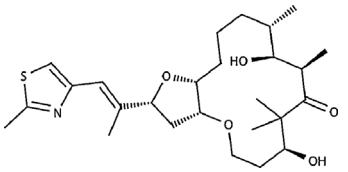	−9.58
17	70	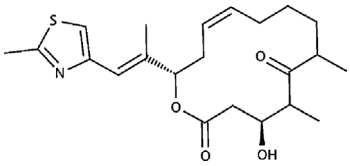	−9.24
21	84	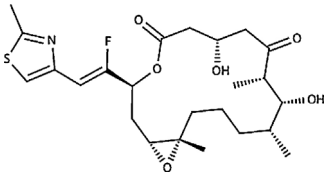	−9.08
22[c]	44	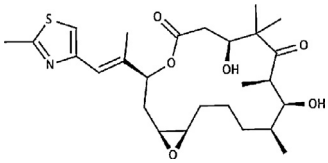	−9.07
23	118	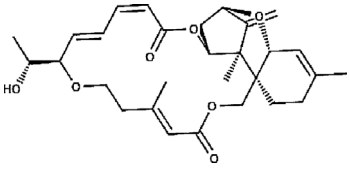	−9.06
24	168	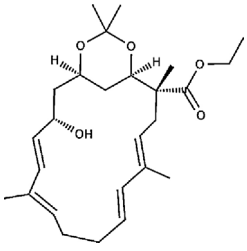	−9.03

[a] These are the IDs that we gave to the molecules.
[b] Binding energy from AutoDock4.2 (kcal/mol).
[c] The positive control, epothilone A.

Table 2
The binding energies of the derivatives of molecule 168203155 in the fifth modification/redocking run.

Rank	ID	Molecule	ΔE [a]
1	1682031551	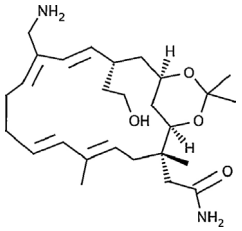	−11.47
2	1682031559	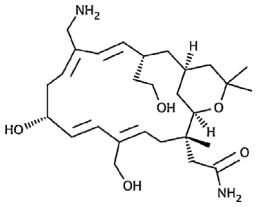	−11.22
3	1682031553	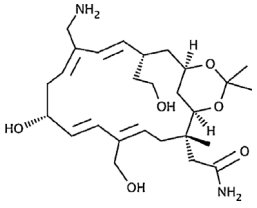	−11.06

[a] Binding energy calculated by AutoDock 4.2 (kcal/mol).

Table 3
Experimental binding constants, K_b, of the five test molecules and the corresponding values of the binding free energies, ΔG^0.

Ligand	K_b (10^7 M^{-1})[a]	ΔG^0 (kcal/mol) [a]
Discodermolide	837 ± 77	−13.6 ± 0.1
Eleutherobin	3.26 ± 0.25	−10.3 ± 0.05
Epothilone A	6.94 ± 1.08	−10.8 ± 0.1
Paclitaxel	2.19 ± 0.05	−10.1 ± 0.01
Sarcodictyin A	0.23 ± 0.09	−8.7 ± 0.2

[a] Data ± standard error; average of at least four independent measurements [12,46].

shows the binding of molecule 1682031551 to β-tubulin where the ligand forms five hydrogen bonds with THR^{274}, ARG^{282}, ARG^{318}, ASP^{26} and ALA^{231}. Such a strong network of hydrogen bonds should help fixing the ligand in position and enhancing its affinity. This could be compared to the hydrogen bond network of epothilone A in β-tubulin, Fig. 4(b), where residues THR^{274}, ARG^{276}, HIS^{227} and ARG^{282} form hydrogen bonds with the ligand as also pointed out by Nettles et al. [29]. THR^{274} and ARG^{282} are residues in common for the two ligands, but ASP^{26}, ARG^{318} and ALA^{231} are specific to our new molecule. This could foretell that the molecule might be effective in epothilone-resistant cell lines.

3.2. Results of rescoring via MM/PBSA

Molecular dynamics simulations were run for the all complexes (five test molecules and three highest-scoring hits). The five test molecules, discodermolide, eleutherobin, epothilone A, paclitaxel and sarcodictyin A, were used as a test for the predictive power of the method. Before using the MM/PBSA script, the five complexes were checked for equilibration of total energy, temperature, density and RMSD and we made sure that they were well-equilibrated. Fig. 5 shows the RMSD equilibration for the five complexes, each of which was equilibrated for at least the last 5 ns of the simulation which was then post-processed using MM/PBSA for binding energy calculation. Enthalpic contribution was calculated using the last 500 evenly spaced snapshots extracted from the last 5 ns. This ensures that each two consecutive snapshots are 10 ps apart and hence uncorrelated. The entropic contribution was calculated using normal mode analysis with 48 evenly spaced snapshots also extracted from the last 5 ns. We could not use more snapshots because normal mode analysis is highly demanding in terms of computational power. The experimental binding constants, K_b, of the five test molecules to the taxol binding site were determined by Buey et al. through displacement of the fluorescent taxoid Flutax-2 [12,46]. These values are presented in Table 3, together with the binding free energies, ΔG°, calculated from the binding constants via the following thermodynamic relationship:

$$\Delta G^\circ = -RT \ln K_b \quad (4)$$

where R is the universal gas constant, $R = 1.987$ cal mol^{-1} K^{-1}, and T is the absolute temperature. The experimentally derived binding energy, ΔG°, for each molecule was plotted against the MM/PBSA

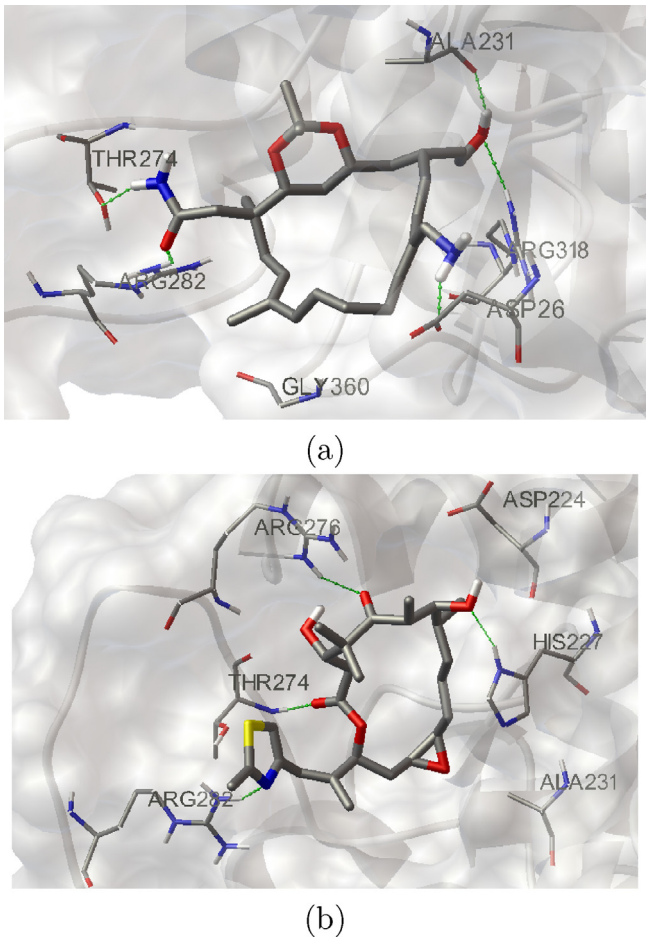

Fig. 4. Ligand binding pose in β-tubulin. (a) Molecule 1682031551 forming five hydrogen bonds with THR^{274}, ARG^{282}, ARG^{318}, ASP^{26} and ALA^{231} and (b) epothilone A forming four hydrogen bonds with THR^{274}, ARG^{276}, HIS^{227} and ARG^{282}.

predicted value as shown in Fig. 6. The figure shows the linear fit of the data which produces and excellent linear correlation with a coefficient of determination, R^2, of 0.99, a slope of 0.2 and an intercept of −4.6 kcal/mol.

This proves that the MM/PBSA protocol that we followed here is a reliable method in predicting the binding energies of the tubulin ligands binding at the taxol binding site and hence can be

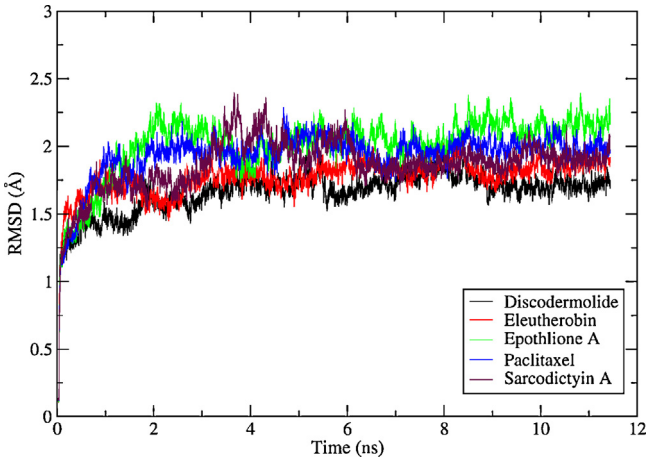

Fig. 5. RMSD equilibration of the five ligand–receptor complexes during an 11 ns simulation run. All molecules have equilibrated at least in the last 5 ns.

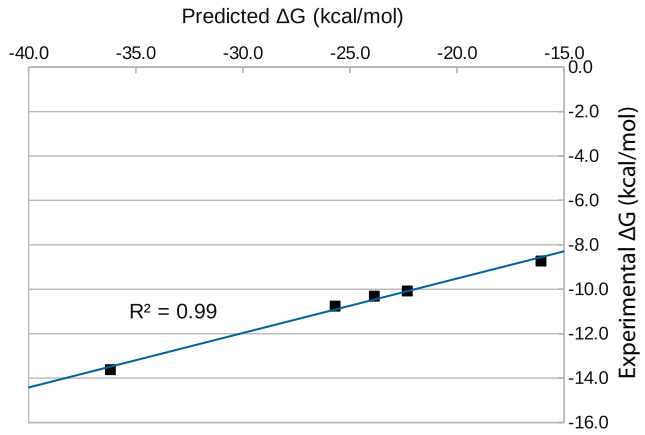

Fig. 6. A linear plot of the MM/PBSA-predicted binding energies versus the experimentally derived values.

carried forward and used to predict the binding energies of the novel hits that we obtained from the screening protocol. Thus, the same MM/PBSA protocol was applied for the three highest-scoring hits shown previously in Table 2, namely molecules 1682031551, 1682031559 and 1682031553. As was done previously with the test molecules, we checked the complexes of these three ligands for equilibration of the total energy, temperature, density and RMSD and made sure that they were all well-equilibrated. Fig. 7 shows the equilibration of RMSD of the three complexes and confirms that the three complexes were equilibrated at least in the last 5 ns. We then post-processed these 5 ns in the same way as the previous complexes and used 500 evenly spaced snapshots for enthalpy calculation and 48 evenly spaced ones for normal mode analysis. The results of this prediction, after extrapolation through the linear fit presented Fig. 6, are shown in Table 4. The results in the table clearly confirm the outcome of the docking experiments and predict that the novel hits may have strong binding energies to the taxol binding site. Molecule 1682031551 shows the lowest predicted binding free energy, −14.7 kcal/mol, which is much lower than all of the test molecules shown in Table 3, all of them being strong tubulin stabilizers. Molecule 1682031553 is also predicted to have a strong affinity of −12.5 kcal/mol toward the taxol binding site which surpasses all of the test molecules except for discodermolide. Finally, molecule 1682031559 is predicted to have an affinity of −10.8 kcal/mol which is still better than paclitaxel,

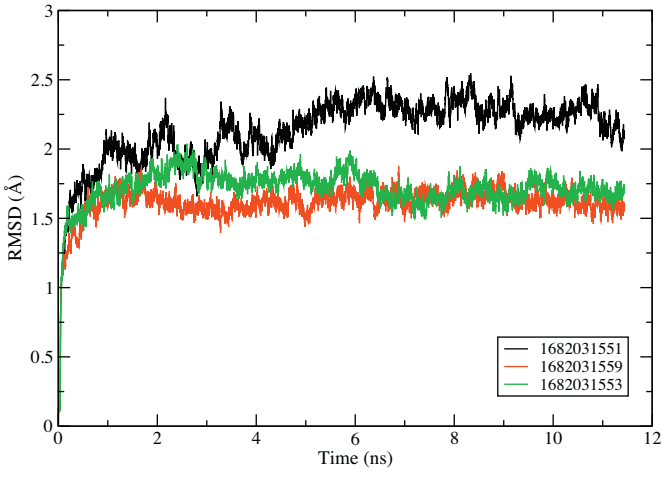

Fig. 7. RMSD equilibration of molecules 1682031551, 1682031559 and 1682031553 during an 11 ns simulation run. All molecules have equilibrated at least in the last 5 ns.

Table 4
Extrapolated binding free energies of top hits as predicted by the MM/PBSA protocol.

Ligand	ΔG (kcal/mol)[a]
1682031551	−14.7 ± 0.9
1682031559	−10.8 ± 0.6
1682031553	−12.5 ± 0.7

[a] Extrapolated value ± standard error based on a 95% confidence interval.

eleutherobin and Sarcodictyin A. In general, these results meet the aim of the study, confirm our findings in the docking runs and show that our novel scaffold could act as a good anticancer tubulin-binding agent.

3.3. Results of physicochemical predictions

After predicting that our new molecules should have high affinity toward the taxol binding site, we checked the physicochemical and toxicological properties of them and compared them to known MSAs to see how our now candidates will compare in terms of drug pharmacokinetics. Table 5 shows the different parameters calculated by ADMET Predictor software. The partition coefficient ($\log P$) is a measure of lipophilicity. It shows that our molecules span a wide range of lipophilicity from 5.33 to 0.94. This is useful since lipophilicity is required for some drugs acting on the brain so that they can pass through the blood-brain barrier which may help with brain tumors. However, too lipophilic compounds might not be soluble in the intestinal fluids and less lipophilic compounds are preferred in this case. The distribution coefficient ($\log D$) is different from $\log P$ for all our four new compounds which shows that they are all ionizable. The effective human jejunal permeability (P_{eff}) decreases with decreasing lipophilicity and spans a wide range from 1.35 to 0.14 μm/s. Interestingly, the solubility in simulated intestinal fluid in fasted state (FaSSIF) is much higher for our new compounds when compared to epothilone A. The solubility of compound 1682031553, for example, is almost 100-fold better than epothilone A, our positive control. Achieving molecules with better solubility was one of the main aims of the study since paclitaxel, for example, is insoluble in water and this was one of its drawbacks [18]. Therefore, the physicochemical profiles of our molecules do achieve one of the aims of this study, that is; finding new tubulin binding candidates with better pharmacokinetic profiles. As to the predicted toxicity of these compounds, all of them showed potential hepatotoxicity, with 1682031559 and 1682031553 showing potential SGOT and SGPT enzyme elevation. Only compound 168203155 showed potential acute rat toxicity. We compared this profile to the predicted profile of our positive control, epothilone A, which showed potential hepatotoxicity and carcinogenicity in rats. Therefore, the toxicological profiles of our molecules and epothilone A are not identical and when carcinogenicity is considered, our molecules may do better than epothilone A as they are predicted to be devoid of this toxic side effect. However, all these are data predicted from simulations, and toxicological assays will indeed be needed to confirm such findings.

Table 5
Predicted physicochemical properties of our newly introduced hits compared to epothilone A.

Ligand	$\log P$	$\log D$	P_{eff} (μm/s)	FaSSIF (mg/mL)
168203155[a]	5.33	3.52	1.35	0.0615
1682031551	3.21	1.55	0.47	0.501
1682031559	1.81	0.35	0.28	1.89
1682031553	0.94	−0.45	0.14	3.99
Epothilone A	3.07	3.07	1.46	0.0433

[a] The parent compound of the fifth run. It is listed here to show how the fifth run affected the lipophilicity of the compounds. See Table 2.

4. Conclusion

The similarity-based virtual screening study reported here predicted five active molecules that have not been patented as tubulin-binding agents before. One of them, molecule 168, is very promising and possesses a novel scaffold. Upon modifying this molecule, optimizing its binding to the receptor and redocking its derivatives in subsequent runs, we managed to obtain several derivatives that are superior to the parent compound, molecule 168, in terms of calculated binding affinity to the target and physicochemical properties. They also showed superiority in binding energy over known tubulin binding agents. Rescoring of the top hits using the MM/PBSA protocol confirmed our findings and showed that at least three of our top hits possess higher binding affinities than the five tubulin stabilizers that were used as query molecules in the similarity-based filtration step. The predicted physicochemical properties of the new compounds also show superiority to the known tubulin stabilizers specially regarding solubility in the intestinal fluid. The toxicological profile predicts comparable toxicity to known MSAs except for carcinogenicity which our new molecules were devoid of. As a follow-up to this study, the next step should be synthesizing these molecules and testing their activities experimentally to confirm the computational findings. It is hope that this work will lead to the development of new and improved cancer chemotherapy compounds.

Acknowledgements

A.A. thanks the university of Alberta for the President's International Doctoral Award. M.K. thanks NSERC for for continuing support. J.T. appreciates the support of the Allard Foundation and the Canadian Breast Cancer Foundation. This research has been enabled by the use of computing resources provided by WestGrid and Compute/Calcul Canada as well as the PharmaMatrix Cluster.

References

[1] A. Jemal, F. Bray, M.M. Center, J. Ferlay, E. Ward, D. Forman, Global cancer statistics, CA: A Cancer Journal for Clinicians 61 (2011) 69–90.
[2] C.M. Croce, Oncogenes and cancer, New England Journal of Medicine 358 (2008) 502–511.
[3] J.H. Hayden, S.S. Bowser, C.L. Rieder, Kinetochores capture astral microtubules during chromosome attachment to the mitotic spindle: direct visualization in live newt lung cells, Journal of Cell Biology 111 (1990) 1039–1045.
[4] P.B. Schiff, J. Fant, S.B. Horwitz, Promotion of microtubule assembly in vitro by taxol, Nature 277 (1979) 665–667.
[5] P.B. Schiff, S.B. Horwitz, Taxol stabilizes microtubules in mouse fibroblast cells, Proceedings of the National Academy of Sciences of the United States of America 77 (1980) 1561–1565.
[6] E. Nogales, S.G. Wolf, K.H. Downing, R.A. Gray, A.M. Pertsov, Structure of the $\alpha\beta$ tubulin dimer by electron crystallography, Nature 393 (1998) 191.
[7] S. Rao, G.A. Orr, A.G. Chaudhary, D.G.I. Kingston, S.B. Horwitz, Characterization of the taxol binding site on the microtubule, Journal of Biological Chemistry 270 (1995) 20235–20238.
[8] S. Rao, L. He, S. Chakravarty, I. Ojima, G.A. Orr, S.B. Horwitz, Characterization of the taxol binding site on the microtubule, Journal of Biological Chemistry 274 (1999) 37990–37994.
[9] D.M. Bollag, P.A. McQueney, J. Zhu, O. Hensens, L. Koupal, J. Liesch, M. Goetz, E. Lazarides, C.M. Woods, Epothilones, a new class of microtubule-stabilizing agents with a taxol-like mechanism of action, Cancer Research 55 (1995) 2325–2333.
[10] E. Hamel, D.L. Sackett, D. Vourloumis, K.C. Nicolaou, The coral-derived natural products eleutherobin and sarcodictyins A and B: effects on the assembly of purified tubulin with and without microtubule-associated proteins and binding at the polymer taxoid site, Biochemistry 38 (1999) 5490–5498.
[11] R.J. Kowalski, P. Giannakakou, S.P. Gunasekera, R.E. Longley, B.W. Day, E. Hamel, The microtubule-stabilizing agent discodermolide competitively inhibits the binding of paclitaxel (taxol) to tubulin polymers, enhances tubulin nucleation reactions more potently than paclitaxel, and inhibits the growth of paclitaxel-resistant cells, Molecular Pharmacology 52 (1997) 613–622.
[12] R.M. Buey, I. Barasoain, E. Jackson, A. Meyer, P. Giannakakou, I. Paterson, S. Mooberry, J.M. Andreu, J.F. Dí az, Microtubule interactions with chemically diverse stabilizing agents: thermodynamics of binding to the paclitaxel site predicts cytotoxicity, Chemistry and Biology 12 (2005) 1269–1279.

[13] O. Pineda, J. Farràs, L. Maccari, F. Manetti, M. Botta, J. Vilarrasa, Computational comparison of microtubule-stabilising agents laulimalide and peloruside with taxol and colchicine, Bioorganic and Medicinal Chemistry Letters 14 (2004) 4825–4829.
[14] M. Khrapunovich-Baine, V. Menon, C.-P.H. Yang, P.T. Northcote, J.H. Miller, R.H. Angeletti, A. Fiser, S.B. Horwitz, H. Xiao, Hallmarks of molecular action of microtubule stabilizing agents: effects of epothilone B, ixabepilone, peloruside A, and laulimalide on microtubule conformation, Journal of Biological Chemistry 286 (2011) 11765–11778.
[15] M.J. Bennett, K. Barakat, J.T. Huzil, J. Tuszynski, D.C. Schriemer, Discovery and characterization of the laulimalide-microtubule binding mode by mass shift perturbation mapping, Chemistry and Biology 17 (2010) 725–734.
[16] G.A. Orr, P. Verdier-Pinard, H. McDaid, S.B. Horwitz, Mechanisms of Taxol resistance related to microtubules, Oncogene 22 (2003) 7280–7295.
[17] K. Natarajan, S. Senapati, Understanding the basis of drug resistance of the mutants of $\alpha\beta$-tubulin dimer via molecular dynamics simulations, PLoS ONE 7 (2012) e42351.
[18] A.K. Singla, A. Garg, D. Aggarwal, Paclitaxel and its formulations, International Journal of Pharmaceutics 235 (2002) 179–192.
[19] E. Hopper-Borge, X. Xu, T. Shen, Z. Shi, Z.-S. Chen, G.D. Kruh, Human multidrug resistance protein 7 (ABCC10) is a resistance factor for nucleoside analogs and epothilone B, Cancer Research 69 (2009) 178–184.
[20] I. Ojima, S. Chakravarty, T. Inoue, S. Lin, L. He, S.B. Horwitz, S.D. Kuduk, S.J. Danishefsky, A common pharmacophore for cytotoxic natural products that stabilize microtubules, Proceedings of the National Academy of Sciences of the United States of America 96 (1999) 4256–4261.
[21] L. He, P.G. Jagtap, D.G. Kingston, H.J. Shen, G.A. Orr, S.B. Horwitz, A common pharmacophore for taxol and the epothilones based on the biological activity of a taxane molecule lacking a C-13 side chain, Biochemistry 39 (2000) 3972–3978.
[22] P. Giannakakou, R. Gussio, E. Nogales, K.H. Downing, D. Zaharevitz, B. Bollbuck, G. Poy, D. Sackett, K.C. Nicolaou, T. Fojo, A common pharmacophore for epothilone and taxanes: molecular basis for drug resistance conferred by tubulin mutations in human cancer cells, Proceedings of the National Academy of Sciences of the United States of America 97 (2000) 2904–2909.
[23] N. Nikolova, J. Jaworska, Approaches to measure chemical similarity: a review, QSAR & Combinatorial Science 22 (2003) 1006–1026.
[24] a. Lipinski, F. Lombardo, B.W. Dominy, P.J. Feeney, Experimental and computational approaches to estimate solubility and permeability in drug discovery and development settings, Advanced Drug Delivery in Reviews 46 (2001) 3–26.
[25] G.M. Morris, R. Huey, W. Lindstrom, M.F. Sanner, R.K. Belew, D.S. Goodsell, A.J. Olson, AutoDock4 and AutoDockTools4: automated docking with selective receptor flexibility, Journal of Computational Chemistry 30 (2009) 2785–2791.
[26] M.D. Hanwell, D.E. Curtis, D.C. Lonie, T. Vandermeersch, E. Zurek, G.R. Hutchison, Avogadro: an advanced semantic chemical editor, visualization, and analysis platform, Journal of Cheminformatics 4 (2012) 17.
[27] D. Case, T. Darden, T. Cheatham III, C. Simmerling, J. Wang, R. Duke, R. Luo, R. Walker, W. Zhang, K. Merz, B. Roberts, S. Hayik, A. Roitberg, G. Seabra, J. Swails, A. Goetz, I. Kolossvry, K. Wong, F. Paesani, J. Vanicek, R. Wolf, J. Liu, X. Wu, S. Brozell, T. Steinbrecher, H. Gohlke, Q. Cai, X. Ye, J. Wang, M. Hsieh, G. Cui, D. Roe, D. Mathews, M. Seetin, R. Salomon-Ferrer, C. Sagui, V. Babin, T. Luchko, S. Gusarov, A. Kovalenko, P. Kollman, AMBER 12, University of California, San Francisco, 2012.
[28] V. Hornak, R. Abel, A. Okur, B. Strockbine, A. Roitberg, C. Simmerling, Comparison of multiple Amber force fields and development of improved protein backbone parameters, Proteins: Structure, Function, and Bioinformatics 65 (2006) 712–725.
[29] J.H. Nettles, H. Li, B. Cornett, J.M. Krahn, J.P. Snyder, K.H. Downing, The binding mode of epothilone A on α, β-tubulin by electron crystallography, Science 305 (2004) 866–869.
[30] J. Wang, R.M. Wolf, J.W. Caldwell, P.A. Kollman, D.A. Case, Development and testing of a general amber force field, Journal of Computational Chemistry 25 (2004) 1157–1174.
[31] A. Jakalian, D.B. Jack, C.I. Bayly, Fast, efficient generation of high-quality atomic charges. AM1-BCC model: II. Parameterization and validation, Journal of Computational Chemistry 23 (2002) 1623–1641.
[32] W. Humphrey, A. Dalke, K. Schulten, VMD – visual molecular dynamics, Journal of Molecular Graphics 14 (1996) 33–38.
[33] P.A. Kollman, I. Massova, C. Reyes, B. Kuhn, S. Huo, L. Chong, M. Lee, T. Lee, Y. Duan, W. Wang, O. Donini, P. Cieplak, J. Srinivasan, D.A. Case, T.E. Cheatham, Calculating structures and free energies of complex molecules: combining molecular mechanics and continuum models, Accounts of Chemical Research 33 (2000) 889–897.
[34] W. Wang, P.A. Kollman, Computational study of protein specificity: the molecular basis of HIV-1 protease drug resistance, Proceedings of the National Academy of Sciences of the United States of America 98 (2001) 14937–14942.
[35] K. Barakat, J. Mane, D. Friesen, J. Tuszynski, Ensemble-based virtual screening reveals dual-inhibitors for the p53-MDM2/MDMX interactions, Journal of Molecular Graphics and Modelling 28 (2010) 555–568.
[36] M. Lepšík, Z. Kříž, Z. Havlas, Efficiency of a second-generation HIV-1 protease inhibitor studied by molecular dynamics and absolute binding free energy calculations, Proteins: Structure, Function, and Bioinformatics 57 (2004) 279–293.
[37] S.P. Brown, S.W. Muchmore, High-throughput calculation of protein–ligand binding affinities: modification and adaptation of the MM-PBSA protocol to enterprise grid computing, Journal of Chemical Information and Modeling 46 (2006) 999–1005.
[38] T. Hou, R. Yu, Molecular dynamics and free energy studies on the wild-type and double mutant HIV-1 protease complexed with amprenavir and two amprenavir-related inhibitors: mechanism for binding and drug resistance, Journal of Medicinal Chemistry 50 (2007) 1177–1188.
[39] ADMET Predictor, Simulations Plus, http://www.simulations-plus.com
[40] D.-S. Su, A. Balog, D. Meng, P. Bertinato, S.J. Danishefsky, Y.-H. Zheng, T.-C. Chou, L. He, S.B. Horwitz, Structure–activity relationship of the epothilones and the first in vivo comparison with paclitaxel, Angewandte Chemie. International Ed. In English 36 (1997) 2093–2096.
[41] S.L. Mooberry, M.K. Hilinski, E.A. Clark, P.A. Wender, Function-oriented synthesis biological evaluation of laulimalide analogs derived from a last step cross metathesis diversification strategy, Molecular Pharmacology 5 (2008) 829–838.
[42] E.E. Lam, S. Goel, L.L. Schaaf, G. Cropp, A. Hannah, Y. Zhou, B. McCracken, B. Haley, R. Johnson, S. Mani, M. Villalona-Calero, Phase I dose escalation study of KOS-1584, a novel epothilone, in patients with advanced solid tumors, Cancer Chemotherapy and Pharmacology 69 (2012) 523–531.
[43] I.H. Hardt, H. Steinmetz, K. Gerth, F. Sasse, H. Reichenbach, G. Höfle, G. Ho, New natural epothilones from *Sorangium cellulosum*, strains So ce90/B2 and So ce90/D13: isolation, structure elucidation, and SAR studies, Journal of Natural Products 64 (2001) 847–856.
[44] M. Sefkow, M. Kiffe, G. Höfle, Derivatization of the C12C13 functional groups of epothilones A, B and C, Bioorganic and Medicinal Chemistry Letters 8 (1998) 3031–3036.
[45] M. Namikoshi, K. Akano, S. Meguro, I. Kasuga, Y. Mine, T. Takahashi, H. Kobayashi, A new macrocyclic trichothecene, 12,13-deoxyroridin E, produced by the marine-derived fungus *Myrothecium roridum* collected in Palau, Journal of Natural Products 64 (2001) 396–398.
[46] R.M. Buey, J. Dí az, J.M. Andreu, A. O'Brate, P. Giannakakou, K.C. Nicolaou, P.K. Sasmal, A. Ritzén, K. Namoto, Interaction of epothilone analogs with the paclitaxel binding site: relationship between binding affinity, microtubule stabilization, and cytotoxicity, Chemistry and Biology 11 (2004) 225–236.